DT# 46762 QA: NA cb 9/11/06

MOL.20061204.0226

Climatic Forecasting of Net Infiltration at Yucca Mountain Using Analogue Meteorological Data

Boris Faybishenko
Earth Sciences Division, Lawrence Berkeley National Laboratory

Abstract

At Yucca Mountain, Nevada, future changes in climatic conditions will most likely alter net infiltration, or the drainage below the bottom of the evapotranspiration zone within the soil profile or flow across the interface between soil and the densely welded part of the Tiva Canyon Tuff. The objectives of this paper are to: (a) develop a semi-empirical model and forecast average net infiltration rates, using the limited meteorological data from analogue meteorological stations, for interglacial (present day), and future monsoon, glacial transition, and glacial climates over the Yucca Mountain region, and (b) corroborate the computed net-infiltration rates by comparing them with the empirically and numerically determined groundwater recharge and percolation rates through the unsaturated zone from published data.

In this paper, the author presents an approach for calculations of net infiltration, aridity, and precipitation-effectiveness indices, using a modified Budyko's water-balance model, with reference-surface potential evapotranspiration determined from the radiation-based Penman (1948) formula. Results of calculations show that net infiltration rates are expected to generally increase from the present-day climate to monsoon climate, to glacial transition climate, and then to the glacial climate. The forecasting results indicate the overlap between the ranges of net infiltration for different climates. For example, the mean glacial net-infiltration rate corresponds to the upper-bound glacial transition net infiltration, and the lower-bound glacial net infiltration corresponds to the glacial transition mean net infiltration. Forecasting of net infiltration for different climate states is subject to numerous uncertainties—associated with selecting climate analogue sites, using relatively short analogue meteorological records, neglecting the effects of vegetation and surface runoff and runon on a local scale, as well as possible anthropogenic climate changes.

1. Introduction

Present-day and potential future net infiltration is a hydrologic parameter that controls the rate of deep percolation, groundwater recharge, radionuclide transport, and seepage into tunnels—which are all, in turn, parameters for the total system performance assessment (TSPA) of the nuclear waste repository at Yucca Mountain, Nevada. Net infiltration is defined as water drainage below the bottom of the evapotranspiration zone within the soil profile or flow across the interface between soil and the densely welded part of the Tiva Canyon Tuff (TCw) at Yucca Mountain. Because net infiltration is largely dependent on climatic conditions, future changes in climatic conditions will potentially alter net infiltration into the deep unsaturated zone (at Yucca Mountain, the depth of the unsaturated zone is on the order of 600 m [Bodvarsson et al., 2003a]).

Although a variety of sophisticated numerical models are being used for predictions of soil infiltration, a key point in selecting an adequate prediction model is to start with the simplest function to describe the structure in the data. Then, if required, more complex models could be used, but they should not be used unnecessarily to preclude generating random noise in the data, which could erroneously be presented as deterministic structure. This will needlessly increase the uncertainty of predictions carried out to answer engineering or scientific questions. Fortunately, many physical systems can be modeled satisfactory with simple analytical or semi-empirical linear or nonlinear functions. The reasonable accuracy of estimates using simple functions is demonstrated in this paper by corroboration of predicted net infiltration rates with the results of other field and modeling studies as obtained from published sources.

Because of the limited amount of meteorological information (such as precipitation, temperature, dew point, and wind velocity records) from meteorologically analogous sites, it is reasonable to apply a relatively simple soil-water-budget approach, which has been broadly used for watershed and regional-scale hydrological and climatological predictions (e.g., Thornthwaite, 1948; Thornthwaite and Mather, 1955; Budyko, 1948; Budyko, 1951; Rasmussen, 1971; Budyko, 1974; Manabe, 1969; Mather, 1978; Alley, 1984; Willmott et al., 1985; Mintz and Walker, 1993; Mintz and Serafini, 1992; Milly and Dunne, 2002). Such an approach has been used successfully for annual (Mather, 1978) and long-term predictions (Brutsaert, 1982).

Conventional models for forecasting changes in water-energy balance usually require using such meteorological parameters as precipitation, solar radiation flux, diurnal and seasonal temperature cycles, evapotranspiration, and relative humidity. However, these parameters are not known for future climates. Therefore, changes in future climatic conditions at Yucca Mountain could be forecasted using meteorological records from analogue meteorological stations (BSC, 2004a,b). In particular, precipitation and temperature can generally be considered as proxy parameters affecting other processes involved in water and energy transfer in an atmospheric-shallow subsurface system (Figure 1).

The objectives of this paper are to: (a) develop a semi-empirical model and forecast average net infiltration rates, using the limited meteorological records from analogue meteorological stations, for interglacial (present day), monsoon, intermediate (glacial transition), and glacial climates over the Yucca Mountain region expected for the next 500,000 years; and (b) corroborate the forecasted net-infiltration rates by comparing them with empirically and numerically determined groundwater recharge and infiltration rates at different field sites as gathered from published data.

The structure of the paper is as follows: Section 2 describes the data characterizing present-day and future climates, reconciling the Desert Research Institute (DRI) (Sharpe, 2002; 2003) and USGS (Thompson et al., 1999; USGS, 2001; BSC, 2004a) reports and records from analogue meteorological stations. Section 3 discusses the conceptual model and main assumptions of the semi-empirical approach used for net-infiltration forecasting for Yucca Mountain's analogue meteorological stations. Section 4 presents the results of calculations of net infiltration and the aridity and precipitation-effectiveness indices for these meteorological stations. Section 5 summarizes the types of uncertainties involved in climatic forecasting of net infiltration and presents the results of corroboration studies in comparison with published data.

Forecasting of net infiltration for different climate states is subject to numerous uncertainties—associated with selecting climate analogue sites, using relatively short records of precipitation and temperature from the analogue meteorological stations, neglecting the effects of vegetation and surface runoff and runon on a local scale, as well as possible anthropogenic climate changes.

However, a detailed analysis of how these factors would affect net infiltration is beyond the scope of this paper.

2. Characterization of Present-Day and Forecasting Future Climates

2.1. Types of Climatic Data and Climate Timing

Characterization of climatic conditions at Yucca Mountain is based mainly on the results of the USGS (USGS 2001; Thompson et al., 1999) and DRI (Sharpe, 2003) paleogeographic and paleoclimatic investigations of the fossil records, specifically the ostracode and diatom assemblages recovered from Owens Lake, California (Sharpe, 2003), and Devils Hole, Nevada (Winograd et al., 1992), as well as Vostok Station, Antarctica (Petit et al., 1999) and orbital cycle periods (Milankovitch theory). Sharpe (2003, Table 6-31, p. T6-33) identified the sequence and duration of past climate states over a period of 500,000 years, including: (1) interglacial climate (IG) (present-day); (2) monsoon (M); (3) intermediate (IM) (glacial transition); (4) glacial 4/2 (G4/2, which corresponds to two equivalent oxygen isotope stages [OIS] 4 and 2), (5) glacial 10/8 (G10/8, which corresponds to two equivalent OIS 10 and 8), and (6) glacial 16/6 (G16/6, which corresponds to two equivalent OIS 16 and 6).

Table 1 presents the duration of past climate states, indicating that the total duration of glacial climate states was 18.3%, with the longest total duration (63.6%) for the IM climate. Brief periods of interglacial peaking typically lasted from a few thousand to perhaps 20,000 years (Muller and MacDonald, 2000). The common approach to forecasting future climate states is based on the assumption that the sequence and duration of past climate states will recur in the future (Knox, 1991). For each climate, Sharpe (2003) identified two types of climatic conditions: the lower-bound climate, causing lower net infiltration; and the upper-bound climate, causing higher net infiltration.

2.2. Present-Day Climate

Both USGS (2001, p. 26) and DRI reports (Sharpe, 2003, Table 6-1, p. 56) indicate the existence of a long-term, present-day interglacial climate state for at least the last 9,000 years before the present. The present-day climate is estimated to last ~600 more years. The present-day meteorological conditions of the Yucca Mountain region feature a mean annual precipitation of 125 mm and a mean annual temperature of 13.4°C for present-day conditions (Thompson et al., 1999, Table 4, Figures 16 and 17). The special distribution of meteorological parameters over the Yucca Mountain region has been characterized using the data collected from a network of nine automated weather stations (BCS, 2004b). However, the meteorological conditions are changing with elevation and time. For example, evidence has recently accumulated that one of the most important features of the present-day climate is that the world climate has begun to warm since the early 1900s. Temperature increased nearly one degree Celsius over the 20th century. Although the causes of this warming are not fully understood, one of the possible reasons for warming is the release of carbon dioxide and other greenhouse gases into the atmosphere (Muller and MacDonald, 2000). The pattern of increasing temperature and precipitation over the past century indicate that the mean temperature and precipitation calculated from the last 30–60 years of observations at analogue meteorological stations may not be statistically representative for the future interglacial climate, if temperature and precipitation continue to increase over time.

2.3. Future Climates

The future interglacial climate states are assumed to be comparable to the relatively warm present-day climate state. The monsoon climate state is characterized by hot summers with increased summer rainfall relative to the present-day climate. This monsoon climate is somewhat similar to the climate in the equatorial region, because of a similar abundant precipitation (rainfall is distributed seasonally as in tropical climates) and temperature regime, even though annual excursion is higher by about 7–8°C. Monsoon climate conditions can presently be found in the southwestern United States (Wright et al., 2001; Cavazos et al., 2002; Douglas et al., 2003).

The glacial-transition climate state has cooler and wetter summers and winters relative to the present-day climate. The future glacial climate is expected to be wetter (pluvial) and cooler than the present-day climate. Most of the last 420,000 years was spent in an ice age, with brief periods of interglacial peaks lasting typically from a few thousand to perhaps 20,000 years (Muller and MacDonald, 2000). According to analogue-based precipitation estimates, the mean annual precipitation for the last glacial maximum was from 266 to 321 mm/yr, which is within the range of the upper-bound present-day precipitation; and the mean annual temperature was 7.9°C to 8.5°C, which is near the lower bound of the present-day temperature range for Nevada District 3 (Thomson et al., 1999).

2.4. Analogue Meteorological Stations' Data

The locations of the analogue meteorological stations for the Yucca Mountain future climates are shown in Figure 2. Individual meteorological stations provide meteorological records, which are obtained at a "point-scale," and for a limited duration of monitoring, only in a few instances exceeding 100 years (Table 2). The relationship between the mean annual precipitation and temperature for present-day, monsoon, intermediate, and glacial climates, using data from analogue meteorological stations, are summarized in Figure 3. The monthly meteorological data for analogue meteorological stations were taken from the database of the Water Regional Climate Center of DRI, Reno, Nevada, at http://www.wrcc.dri.edu/.

The precipitation and temperature data from the analogue meteorological stations are assumed to be constant for each climate state. In other words, these data do not take into account the dynamic pattern of temperature changes over time, as determined from the Devils Hole (Winograd et al., 1999) and Vostok ice core (Muller and McDonald, 2000) data analysis.

3. Soil-Water-Balance Model and Calculations of Net Infiltration Using Climatic Data

3.1. Soil-Water Balance and Main Assumptions

Semi-empirical formulae are generally good predictors for large-scale characterization of soil moisture balance (Rasmussen, 1971; Milly and Dunne, 2002). The general form of the water-balance equation for the evaluation of net infiltration can be given by:

$$I_n = P - ET - S - R_{off} + R_{on} \tag{1}$$

where I_n is the net infiltration, P is the total precipitation, including the snowmelt, ET is the evapotranspiration, S is the soil water change in storage, R_{off} is the runoff, and R_{on} is the runon.

Time and depth intervals of the soil/rock profile, for which the components of Equation (1) are calculated, are generally dependent on the investigation objectives. The time step may vary from one day to tens of years or longer, and the depth may vary from the topsoil depth to the depth of seasonal fluctuations of moisture content or the depth of evapotranspiration.

It is well-known that for arid and semi-arid climatic conditions, annual potential evapotranspiration exceeds the precipitation. Despite large values of net radiation (largely affecting potential evapotranspiration) at Yucca Mountain, episodic infiltration (of precipitated and snowmelt water) into the subsurface may cause preferential and transient flow through the upper portion of a deep unsaturated zone (Scanlon et al., 1997). Walvoord et al. (2002b) incorporated into their vapor transport model observations of temporally invariant matric potentials at 3–5 m depths over ~5 year monitoring periods, and simulated the presence of net upward water movement from 3 to ~10 or 20 m depths. Yet, the conventional chloride mass balance approach indicated an overall downward advective liquid flux into a deep unsaturated zone.

In general, all terms of Equation (1) are likely to vary over time, as affected by changes in climatic conditions. Using the water-balance approach, which is developed for large-scale investigations (Dooge, 1988), we assume a steady-state (time-averaged) net-infiltration regime for each climate. The errors that could be caused by this assumption should be further evaluated, because modeling of the coupled liquid-gas-heat movement through a deep unsaturated zone in arid environments indicates the presence of unsteady water flow even after 10–15 kyr of continuous drying (Walvoord et al., 2002a). For the first-order estimation of long-term average net infiltration for future climates, we also assume (a) soil water storage does not change, and (b) lateral water motion within the shallow subsurface is negligible, and (c) the terms of the surface water runoff and runon in a regional scale water-balance model simply cancel each other out and need not be included in the large-scale, regional water-balance model for the net-infiltration estimation. The latter is based on the results of field monitoring within the arid and semi-arid areas of the southwestern United States, indicating that stream runoff at the mountain front is generally ephemeral and almost always disappears within the mountain front zone. Consequently, downstream runoff beyond the mountain front could be considered negligible, leading to a simplification of the water-balance model (Wilson and Guan, 2004). The surface runoff and runon are likely to affect net infiltration at the local scale, such as the crest of Yucca Mountain, and could be changed with changes in climatic conditions. However, the estimates of surface runoff and runon under the influence of climate are beyond the scope of this study. Therefore, in our study, we assume that the surface runoff and runon within the watershed cancel each other, so that all surplus water presents a source of net infiltration.

3.2. Semi-Empirical Budyko's Hydrological Model

For long-term estimates, at least for 1 year, assuming that the change in moisture storage in soil and the net ground heat flux are small, and that a sensible heat flux is positive, the evapotranspiration, E, can be expressed as a function of the aridity index, $\phi = E_0/P$, where E_0 is the potential evapotranspiration (Arora, 2002):

$$E = P\,f(\phi) \tag{2}$$

Budyko (1974) used net radiation as a surrogate for potential evapotranspiration E_0, and stated that if $E_0=R/L$ (where R is the net radiation, and L is the latent heat of evaporation) then the following conditions should satisfy:

for dry soils $E/P \rightarrow 1$ as $R/LP \rightarrow \infty$, and
for moist soils $LE \rightarrow R$ at $R/LP \rightarrow 0$.

These conditions would determine the form of the function $f(\phi)$. Several formulae were developed to describe the empirical relationship between precipitation and the aridity index. Schreiber (1904) was probably the first who proposed an exponential relationship to express the relation between E, P, and the aridity index, ϕ, given by:

$$E/P = 1\text{-}\exp(-\phi) \tag{3}$$

Then Ol'dekop (1911) developed a hyperbolic tangent relationship given by:

$$E/P = \phi\,[\tanh(1/\phi)]. \tag{4}$$

Using the water-balance data from a number of catchments around the world, Budyko (1974) found that empirical data were scattered between the curves described by the exponential relationship (3) of Schreiber (1904) and the hyperbolic tangent relationship (4) of Ol'dekop (1911). To describe experimental data, Budyko (1974) employed the geometric mean of the right-hand sides of (3) and (4) given by:

$$E = \left[\frac{RP}{L}\tanh\frac{LP}{R}\left(1-\cosh\frac{R}{LP}+\sinh\frac{R}{LP}\right)\right]^{0.5} \tag{5}$$

or in a simpler form:

$$E/P = \{\phi\tanh(1/\phi)\,[1-\exp(-\phi)]\}^{0.5} \tag{6}$$

Equation (6) was initially tested for 29 European river basins (Budyko, 1951) and then for 1,200 regions with known precipitation and runoff data (Budyko and Zubenok, 1961). Although the original Budyko's model was developed for the determination of the surface runoff, the Budyko-like approach was also used to assess an infiltration-runoff component of the water balance and the catchment-scale soil moisture capacity (Potter et al., 2005). Several papers have been published in which the authors described experimental data obtained on the watershed scale using various relationships analogous to that of Budyko. For example, Milly and Dunne (2002) conducted their studies for large river basins (10,000 km^2 and greater); Sankarasubramanian and Vogel (2002) incorporated the soil moisture storage capacity into their Budyko-like model, based on the results of observations at 1,337 watersheds throughout the U.S. with at least ten years of records.

Several other Budyko-like models have been used for hydrological calculations. For example, the generalized Turc-Pike equation is given by

$$E/P = [1 + (1/\phi)^2]^{-0.5} \quad (7)$$

and was tested using data from 250 catchments from different climatic zones (Pike, 1964). (In the original Turc [1954] equation the 1st coefficient is 0.9.) Zhang et al. (2001) implemented the "plant-available water coefficient" (introduced by Milly, 1994) to represent the soil moisture transpiration by plants. The rational function equation developed by Zhang et al. (2001) is given by

$$E/P = (1 + w\phi)/(1 + w\phi + \phi^{-1}) \quad (8)$$

where w is the plant water-availability coefficient, which is proportional to the root zone depth. To take into account Budyko's idea of using net radiation to represent the value of potential evaporation, Zhang et al. (2001) used the Priestly and Taylor (1972) formula for calculating E_o.

Figure 4 shows close agreement between various curves relating the evaporation ratio (E/P) and the aridity index, $\phi=E_o/P$, using the Budyko (1974), Turc (1954), and Zhang et al. (2001) formulae. This figure shows two curves calculated using the Zhang et al. (2001) formula, given by Equation 8: for w=0.5 (for pasture) and w=2 (for forests). The statistical analysis of curves shown in Figure 4 indicates that the mean relative error when using Budyko's curve is only 0.7%, in comparison with the average of all other curves shown in Figure 4. An example of the comparison of experimental data and calculated curves from the Zhang et al. (2001) paper is shown in Figure 5.

Figures 4 and 5 show that the E/P versus ϕ curves approach unity asymptotically, as the aridity index increases. The straight segments A and B reflect the physical constraints of a water-balance model: The straight line A presents an asymptote for energy-limited evapotranspiration, and the straight line B presents an asymptote for water-limited evapotranspiration. The annual and seasonal cycling of climate may cause the transition between segments A and B (Budyko and Zubenok, 1961; Milly, 1994; Milly and Dunne, 2002).

Budyko and Zubenok (1961), who tested Budyko's model using the data from 1,200 regions, show that the mean discrepancy between the evapotranspiration calculated from Equation (6) and that derived by the water balance was about 10%. Budyko (1974) also stated that this relationship could be applied to most mountainous basins (but not for the highest mountain basins) and to watersheds with runoff that does not vary appreciably over the area. The departure from the classical Budyko curve could be caused by biases in estimations of precipitation, discharge, net radiation or potential evaporation, and human disturbance of natural water fluxes in arid basins (Milly and Dunne, 2002).

Although Budyko (1974) hypothesized that radiative energy supply is equivalent to the upper bound of the latent heat flux, Milly and Dunne (2002) showed that actual evaporation could exceed that determined from net radiative energy supply. Milly and Shmakin (2002, p. 302) indicated that "[O]veral, no model performed substantially better than Budyko's equation, and most models performed much worse. The superieor performance of Budyko's equation was found despite the fact that most or all of the models had the advantage of using information on the global distribution of surface characteristics."

3.3. Semi-Empirical Model for Net Infiltration

Based on the assumptions introduced in Section 3.1, for large spatial and long-term temporal scales, all surplus water calculated from the water-balance equation will leave the system as net infiltration, which can be determined from:

$$I_n=P\,[1-f(\phi)] \qquad (9)$$

or

$$I_n/P=1-f(\phi) \qquad (10)$$

where the ratio I_n/P can be called a net infiltration index (dimensionless value or a percent of the total precipitation—the sum of precipitation and snowmelt). Using $E/P=f(\phi)$ calculated from Equation (6), as an example, Figure 6 demonstrates the variations of net infiltration for different values of potential evapotranspiration E_0. The approach to calculating the value of E_0 for the evaluation of the aridity index is described in Section 3.3.

3.3. Evaluation of Reference Potential Evapotranspiration

3.3.1. Rationale for Selecting a Method for the Evaluation of E_o

Evapotranspiration is a dominant water-balance component in arid and semi-arid areas, which combines bare-soil evaporation and transpiration by plants. The potential evapotranspiration is often determined using various experimental methods and mathematical formulae, which, however, may often produce inconsistent results (Lu et al., 2005), especially for interannual predictions (Sankarasubramanian and Vogel, 2002). The determination of evapotranspiration is particularly difficult for mountain areas with varying elevation, vegetation, and runoff areas (Wilson and Guan, 2004). Furthermore, significant uncertainty and ambiguity in estimating potential evapotranspiration are caused by limited meteorological data (Brutsaert, 1982).

Three common approaches to evaluating evapotranspiration are through (a) energy budget, (b) aerodynamics, and (c) temperature. With the energy-budget approach, the net radiation available at the surface (shortwave absorbed plus longwave emitted) must be partitioned between latent heat flux and sensible heat flux, assuming that ground heat flux is negligible. This approach is typically based on using the Bowen ratio, which requires measurements of temperature and humidity at two different heights. The aerodynamic approach typically involves evaluation of a vapor transport coefficient and vapor pressure gradient between the saturated surface and an arbitrary measurement height, and the determination of wind speed, humidity, and temperature. For example, Penman (1948), combining the energy-budget and aerodynamic approaches, developed an equation using a weighted average for the rates of evaporation caused by net radiation and turbulent mass transfer.

Depending on the goal of investigations, semi-empirical methods used for the evaluation of potential evapotranspiration can be grouped into two categories: (1) reference-surface potential evapotranspiration (for example, temperature-based Hargreaves-Samani, Thornthwaite, Hamon, Jensen-Haise, and Turc models, and radiation-based Priestly-Taylor and Penman methods), and (2) surface-dependent potential evaporation (for example, radiation-based Penman-Monteith and Shuttleworth-Wallace methods). The reference-surface potential evapotranspiration is defined as evapotranspiration that would occur from a land surface with a "reference crop," which is usually a short, uniform, green plant cover (such as alfalfa or grass) under designated weather conditions and well-moist soil (Federer et al., 1996; Shuttleworth, 1991). Although empirical reference-surface E_o

relationships take into account the effect of meteorological factors, they do not explicitly include the effect of vegetation. The surface-dependent E_0 depends on the surface and aerodynamic resistances, which are used to account separately for transpiration and soil evaporation. Because the reference-surface E_0 is a climatic parameter, which is computed from meteorological data, it expresses the evaporation rate generated by the atmosphere at a specific location and time, with no effects of crop characteristics and soil factors (Allen et al., 1998).

To calculate reference-surface potential evapotranspiration to represent the effect of net radiation in the Budyko model, this investigator used the Penman (1948) model, which is known to produce accurate results (Thom et al., 1981; ASCE, 1990). Another reason for using this formula is the fact that the WRCC database contains practically all meteorological parameters from observations at analogue meteorological stations, which are needed for calculations using the Penman model. The meteorological records in the WRCC database contain the following types of average-monthly data, which we used in our calculations: total precipitation (precipitation plus snow melt); minimum, maximum, and mean air temperature; dew point temperature; wind speed; solar radiation; and pan evaporation (determined using Class A pan evaporometers). The types of meteorological data used in our calculations are summarized in Table 2.

3.3.2. Estimates of Reference-Surface Potential Evapotranspiration

3.3.2.1. Penman Model

Penman's equation (Penman, 1948) combines the two main processes affecting the evaporation rate, or evapotranspiration rate from a well watered surface: (a) the energy input, and (b) the aerodynamic exchange between the surface and atmosphere. Accordingly, the common two-term form of the Penman (1948) equation for the evaluation of E_0 is given by

$$E_o = \frac{\Delta}{\Delta + \gamma}(R_n - G) + \frac{\gamma}{\Delta + \gamma}E_a \qquad (11)$$

where Δ is the slope of the saturation vapor pressure-temperature curve, γ is the psychometric constant, R_n is the net radiation expressed in water-depth units (equivalents of energy), G is the soil heat flux, which can be assumed zero for annual (or longer) predictions, and E_a is the aerodynamic transport term, which is commonly given by

$$E_a = f(u)(e_s - e_d) \tag{12}$$

where $f(u)$ is the wind speed (u) function, e_s is the saturation vapor pressure, and e_d is the saturation vapor pressure corresponding to the dew point temperature. Various forms of the wind function $f(u)$ (depending on crop types, the height of measurements, and other factors) are described by Hatfield and Allen (1996). In this study, we used the function

$$f(u) = 2.63\ (a + bu) \tag{13}$$

with coefficients a=1 and b=0.56, originally proposed by Penman. The Penman formula estimates reference-surface evapotranspiration from nonvegetated (or sparsely vegetated) areas.

Assuming that under abundant water-supply conditions evapotranspiration would eventually attain an equilibrium rate, the actual evapotranspiration rate would be equal to the Penman potential evapotranspiration. Priestley and Taylor (1972) expressed the effect of the aerodynamic term introduced in the Penman equation using a factor (α) equal to 1.26. However, this factor could vary depending, for instance, on the surface roughness and soil moisture content, and may underestimate both peak and seasonal evapotranspiration in arid climates, because of neglecting the advection term in the heat balance equation.

In areas with no or small water deficit, approximately 95% of the annual evaporative demand is supplied by radiation (Stagnitti et al., 1989). Shuttleworth and Calder (1979) reported that the difference in estimates of E_0 produced using Penman and Priestly-Taylor equations is within approximately 5% of each other. Although the Penman equation may produce the accurate results (ASCE, 1990, p. 249), uncertainties of meteorological data for future climates may create commensurate uncertainty in predicting potential evaporation for future climates. (Note that Penman formula estimates of E_0 closely match those from Class A pan evaporometers with corrections involving the pan adjusted coefficient for dry areas—see Section 5.2).

3.3.2.2. Conversion of Pan Evaporation to Reference Evapotranspiration

Direct measurements of the evaporation rate from shallow water pans at meteorological stations are commonly used for estimating potential evaporation. Evaporation-pan rates depend on the pan's geometry, latitude, elevation, solar declination, and the cloud coverage, and usually overestimate the potential evapotranspiration under arid climate conditions (Linacre, 1994; Allen et al., 1998). Evaporation pans may give reasonable estimates of potential evapotranspiration in humid regions. To obtain realistic estimates of potential evapotranspiration in arid climate, the results of pan evaporation measurements should be adjusted by taking into account the pan's geometry, environmental setting, and operation conditions (Rosenberg et al., 1983; Allen et al., 1998). Pan coefficients also depend on the size and state of the upwind buffer zone (fetch): the larger the upwind buffer zone, the more the air moving over the pan will be in equilibrium with the buffer zone. The equation for the evaporation-pan adjustment coefficient for dry fetch (which is more likely to represent the nonvegetated or sparsely vegetated Yucca Mountain area) is given by (Allen et al., 1998, Chapter 4):

$$K_p = 0.61 + 0.00341 RH_{mean} - 0.000162\, u_2\, RH_{mean} - 0.00000959\, u_2\, FET + 0.00327\, u_2 \ln(FET) - 0.00289\, u_2 \ln(86.4\, u_2) - 0.0106 \ln(86.4 u_2) \ln(FET) + 0.00063 [\ln(FET)]^2 \ln(86.4\, u_2) \quad (14)$$

where RH_{mean} is the mean relative humidity, u_2 is the wind speed at the 2 m elevation, and FET is the fetch distance, which varies from 50 m to 2,000 m. In our calculations, FET was 1,000 m. The K_p values vary typically from 0.5 to 1.0. It will be illustrated in Section 5.2 that calculations of E_o using Penman's formula for Yucca Mountain analogue meteorological stations show a good agreement with the corrected values of E_o determined using Class A evaporometers, as well as Priestly-Taylor's formula.

3.4. Precipitation-Effectiveness Index

Using precipitation and temperature as proxy representing climatic processes, the moisture conditions can be characterized using the Thornthwaite precipitation-effectiveness (*P-E*) index (NAM, 2002). The *P-E* Index is calculated using monthly precipitation and temperature values (Thornthwaite, 1931):

$$P\text{-}E \text{ Index} = 10\sum(P\text{-}E \text{ ratio})_n \qquad (15)$$

where monthly *P-E* ratio being $11.5P/(T\text{-}10)]^{10/9}$, P is average monthly precipitation (inches) (with 0.5 being the minimum value), T is average monthly temperature (^{o}F) (minimum temperature of 28.4^{o}F is used in calculations), and summation is provided for 12 months of the year. (The results of calculations of the relationship between the *P-E* and net-infiltration indices are given in Section 4.2)

4. Results of Calculations

4. 1. Net infiltration for Analogue Meteorological Stations

Table 3 presents the results from calculating the potential evapotranspiration and net infiltration for different climates. Using the calculated net infiltration rates, Figure 7 illustrates the relationship between net infiltration, I_n, and the mean annual precipitation, P_m (both are in mm per yr) given by

$$I_n = 4 \times 10^{-9}\, P_m^{\,3.92} \qquad (16)$$

with $R^2 = 0.93$.

Figure 8 present the plots of climatic ranking of the net-infiltration index (% of precipitation) and net infiltration rates (in mm/yr). These plots demonstrate a general trend of increasing net infiltration from the present-day climate to monsoon, glacial transition, and then to glacial climate. For the glacial climate, net infiltration during the G16/6 climate (its duration is only 2.5% of the total duration of future climates—see Table 1) ranges from 39.9 to 213 mm/yr, which exceeds the net-infiltration ranges for the other two glacial climates. Net infiltration for the G4/2 climate (its duration is 7.3% of the total duration of future climates) is from 5.5 to 71.1 mm/yr, and it overlays the lower bound of the G16/6 net infiltration. At the same time, it roughly corresponds to the net infiltration rate for the glacial transition climate. The G10/8 (its duration is 8.5% of the future climates) net infiltration rate generally exceeds that for the G4/2 climate; its lower bound is within that for the glacial transition climate, and its upper bound exceeds that for the glacial transition. Overall, the mean infiltration rate of the glacial climate corresponds to the upper bound of the glacial transition climate, which is 100 mm/yr.

4.1.2. Aridity and *P-E* indices

The aridity index can be used to classify climatic regimes (Ponce et al., 2000): arid ($12>\phi\geq5$), semi-arid ($5>\phi\geq2$), subhumid ($2>\phi\geq0.75$), and humid ($0.75>\phi\geq0.375$). Figure 9a depicts the ranking of the annually average aridity indices, which is generally consistent with that from the net-infiltration ranking shown in Figure 8. Figure 9a shows that for the present-day climate, the aridity index ranges from that typical for arid (lower-bound arid climate net infiltration) and semi-arid climates (upper-bound arid climate net infiltration); the monsoon climate is characterized by the aridity index spanning from the arid climate (low-bound monsoon infiltration) to lower border between the semi-arid and subhumid climates (upper-bound monsoon net infiltration). For the intermediate (glacial transition) climate, the aridity index spans the range from the middle of the semi-arid climate to the low aridity subhumid indices. Finally, for the glacial climate, the aridity index is mostly within the range typical for subhumid climate, and it even decreases to that for humid climate for the G16/6 climate.

Climatic ranking of the *P-E* indices, shown in Figure 9b, is essentially the same as that of the net-infiltration indices, because there is virtually a linear relationship between the *P-E* and net-infiltration indices. Figures 9c and 9d show the fitting curves for the net-infiltration versus the *P-E* and aridity indices, which can be used for forecasting net infiltration if these indices are known.

5. Corroboration of the Forecasting Results

5.1. Sources of Uncertainties and Approach to Corroboration

An often encountered difficulty in the evaluation of model-predicted components of the water balance, including evapotranspiration and net infiltration, is the lack of widespread field observations that can be used to compare model predictions at the spatial and temporal scales. It is apparent that a significant error (or uncertainty) in evaluating net infiltration from the regional water-balance model could result from net-infiltration being the smallest component of the water-balance equation. In other words, net infiltration is computed as the difference between other, much greater values of the water-balance equation (e.g., precipitation, evapotranspiration, and runoff/runon). Moreover, the difficulty in validating computed values of net infiltration for future climates arises from there being no reliable direct (field) measurements of net infiltration at Yucca Mountain representing different climatic conditions.

As part of establishing confidence in the results of this study, this investigator corroborated the approach developed here by comparing the results of evapotranspiration and net-infiltration calculations with other independently determined estimates. In Section 5.2, the estimates of E_0 from Penman formula will be compared with measurements conducted using Class A evaporation pans and calculations using Priestly-Taylor formula for different meteorological stations. In Section 5.3, the estimates of net infiltration will be compared with local and area-averaged groundwater recharge and percolation rate data from different sites, using published data.

5.2. Comparison of Computed and Experimentally Determined Evapotranspiration Rates

To establish confidence in the results of the evaluation of the reference surface-potential evapotranspiration, we will compare the estimates of potential evaporation using Penman (1948) and Priestly-Taylor (1972) formula with field observations conducted using Class A evaporation pans at different meteorological stations. The measured Class A evaporation rates were corrected using the correction coefficient suggested in FAO56 recommendations for dry surfaces (Allen et al., 1998, Chapter 4)—see Section 3.3.2.2. Figure 10 illustrates a good agreement between the estimates using semi-empirical Penman and Priestly-Taylor formula and corrected evaporation pan measurements for analogue meteorological stations. Our results correspond to the conclusions of comprehensive experimental and theoretical studies by Thom et al. (1981), who showed a good comparison of the results of corrected evaporation pan measurements with those computed using the Penman formula.

The author will present, in a separate paper, a detailed analysis and a comparison of estimates of potential evapotranspiration using Blaney-Criddle, Hargreaves-Samani, Priestly-Taylor, Penman, Penman-Monteith, Turc-Pike, Thornthwaite, Jensen-Haise, Caprio, Linacre, Makkink, Hansen, and Bair-Robertson formula, along with adjusted Class A pan evaporometer data for the State of Nevada and the Yucca Mountain future climate analogue meteorological stations.

5.3. Comparison of Net Infiltration with Groundwater Recharge

Comparison of calculated net infiltration with empirically determined groundwater recharge rates, at analogue sites in arid and semi-arid areas, is a valuable approach to building confidence in the results of climatic net-infiltration forecasting at Yucca Mountain. The use of this approach is based on the assumption of steady-state water flow through the unsaturated zone, in spite of the results of modeling that show that deep flow and transport processes are still responding slowly to large shifts in Pleistocene-Holocene climatic and vegetation changes that occurred about 10,000–15,000 years ago (Walvoord et al., 2002b).

One of the widely used methods for estimating recharge is the Maxey-Eakin method (Maxey and Eakin, 1950). This method was used in several previous water-balance studies of the Death Valley region to estimate groundwater basins' recharge. According Maxey and Eakin (1950): (1) for precipitation less than 203 mm/yr, no groundwater recharge occurs, (2) for precipitation from 203 to 304 mm/yr, groundwater recharge is 3% (this estimate corresponds to the results of the water-balance calculations of discharge measurements from springs south of Yucca Mountain near the Nevada–California border by Winograd and Thordarson [1975]), (3) for precipitation from 305 to 380 mm/yr—groundwater recharge is 7%, (4) for precipitation from 381 to 507 mm/yr, groundwater recharge is 15%, and for precipitation of 508 mm/yr and greater, groundwater recharge is 25%. The Maxey–Eakin recharge rates were determined from groundwater balance estimates of the recharge and discharge, depending on the depth to the water table, for 13 valleys in east-central Nevada. By comparing the Maxey–Eakin estimates with 40 estimates of recharge obtained from the Southern Great Basin, using a basinwide water-budget analysis, and 27 estimates of recharge obtained using geochemical and numerical modeling approaches, Avon and Durbin (1994) and Harrill and Prudic (1998) concluded that the Maxey–Eakin method provides reasonable estimates of recharge for basins in Nevada. Several studies have presented modified and updated versions of the Maxey–Eakin method, based on recent precipitation data, geochemical data, and basinwide water-balance data (D'Agnese et al., 1997; Donovan and Katzer, 2000).

In the Maxey–Eakin method, the areas with annual precipitation of less than 200 mm are not considered to recharge the groundwater. However, at Yucca Mountain, recharge is known to occur within areas where annual precipitation is less than 200 mm. Therefore, the comparison of the calculated net infiltration with that from the Maxey–Eakin coefficients for the annual precipitation of less than 200 mm is invalid. Moreover, estimates of net infiltration for the Yucca Mountain area may not correspond directly to recharge because of the time lag between the net infiltration and groundwater recharge in the thick unsaturated zone.

Figure 11 summarizes the results of comparing forecasted net infiltration for analogue meteorological stations with estimation of groundwater recharge determined using various independent field methods and modeling, including:

(1) The Maxey-Eakin (M-E) recharge rates;

(2) Groundwater recharge estimates, using a chloride-balance method, for two small, upland watersheds in central and south-central Nevada—310 mm/yr, or about 50% of the estimated average annual precipitation of 639 mm, and 33 mm/yr, or 9.8 percent of the average precipitation of 336 mm/yr (Lichty and McKinley 1995, Table 15);

(3) Groundwater recharge rates for Fenner Basin of the Eastern Mojave Desert, California (Davisson and Rose, 2000);

(4) Assessments of mountain front recharge for various locations—from Table 2 of Wilson and Guan (2004);

(5) Groundwater recharge rates for Huntington Valley in northern Nevada (Czarnecki, 1985);

(6) Groundwater recharge rates for northeastern Arizona determined from ^{14}C and chloride data (Zhu, 2000);

(7) An empirical power-law relationship given by Wilson and Guan (2004):

$$R_g = 9 \times 10^{-9} P_m^{3.72} \quad (17)$$

where R_g is the groundwater recharge, P_m is the mean annual precipitation (both R_g and P_m are in millimeters per year). Figure 11 shows that this equation deviates from Maxey-Eakin estimates for $P_m > 600$ mm/yr.

(8) An empirical power-law regression for subsurface flow and surface runoff in mountain areas, which potentially become the groundwater recharge, at Carson Basin, Nevada, given by Maurer and Berger (1997):

$$R_g = 2.84 \times 10^{-5} P_m^{2.43} \quad (18)$$

In Equation (18), R_g and P_m are also in millimeters per year. Figure 11 shows calculations using this equation exceed the results of the Maxey-Eaking estimates for $P_m<350$ mm/yr.

To provide confidence in the results of calculations of net infiltration, Figure 8 (lower panel) also includes the estimates of percolation rates through the Yucca Mountain unsaturated zone from several independent corroborative studies: chloride mass balance—from 0.73 to 10.6 mm/yr (Liu, J. et al. 2003), calcite data—from 2 to 6 mm/yr (Xu et al. (2003), temperature measurements in boreholes at the crest of Yucca Mountain—5-10 mm/yr (Bodvarsson et al. 2003b); and the results of the experts' evaluation of net infiltration—from 3.9 to 12.7 mm/yr (CRWMS M&O 1997b).

Thus, Figures 8 and 11 demonstrate that computed net infiltration rates versus precipitation for analogue meteorological stations correspond relatively well to independently determined empirical and numerical estimates of groundwater recharge and infiltration rates from published data.

6. Summary and Conclusions

It is essential to forecast the range of (or to bound) net infiltration over the Yucca Mountain area—for both the present-day climate state and future climate conditions representing the monsoon, glacial transition, and glacial climates—to assess long-term repository performance. These climate conditions are represented using temporally limited meteorological records of monthly averaged total precipitation, temperature, solar radiation, dew point temperature, and evapotranspiration from analogue meteorological stations at Yucca Mountain.

The developed semi-analytical model is based on computing net infiltration from Budyko's empirical water-balance model, using the estimates of reference-surface potential evapotranspiration from the Penman (1948) formula (for the analogue meteorological stations, the estimates of potential evapotranspiration from the Penman formula are in close agreement with Priestly-Taylor and adjusted Class A pan evaporation measurements).

The results of calculations were used for ranking net infiltration, along with aridity and precipitation-effectiveness indices, for future climatic scenarios. We determined a general power law trend of increasing net infiltration from the present-day climate to monsoon, to intermediate (glacial transition), and then to glacial climates. The ranking of the aridity and *P-E* indices is practically the same as that of net infiltration. The calculated net-infiltration rates for the Yucca Mountain analogue meteorological stations have yielded a good match with other field and modeling study results pertaining to groundwater recharge, percolation flux through the unsaturated zone, and net-infiltration evaluation. This comparison indicates the robustness of the simple water-balance approach used in this paper.

Future research should include the evaluation of uncertainties related to selecting analogue meteorological sites spanning the anticipated range of meteorological conditions within each climate state, calculations using relatively short meteorological records (for example, only precipitation and temperature) from the analogue stations, and accounting for possible anthropogenic climate changes. Future research should also include the evaluation of uncertainties and deviations from the regional scale Budyko curve (Potter et al., 2005) as affected by the soil plant-available water-holding capacity, various seasonality parameters (Milly, 1994), vegetation and plant-available water coefficient (Zhang et al., 2001), soil-moisture storage capacity (Rasmussen, 1971; Sankarasubrumanian and Vogel, 2002), the effect of surface runoff (Rasmussen, 1971; Sharif and Miller, 2006), and anthropogenic climate effects. Since infiltration rates affect the percolation flux though the unsaturated zone and groundwater recharge, it would be desirable to perform an uncertainty analysis to address how sensitive unsaturated and saturated zone contaminant transport are to the variability of infiltration.

Acknowledgments: This work was supported by the Director, Office of Civilian Radioactive Waste Management, U.S. Department of Energy, through Memorandum Purchase Order EA9013MC5X between Bechtel SAIC, LLC, and the Ernest Orlando Lawrence Berkeley National Laboratory (Berkeley Lab). The support is provided to Berkeley Lab through the U.S. Department of Energy Contract No. DE-AC03-76SF00098. The author thanks Stefan Finsterle, H.H. Liu, Norman Miller, and Dan Hawkes of LBNL for review of this paper. The author appreciates very much the review comments by three anonymous reviewers.

References

Alley, W.M., On the treatment of evapotranspiration, soil moisture accounting, and aquifer recharge in monthly water balance models, *Water Resources Research*, 20,1137-1149,1984.

Allen, R.G., Pereira, L.S., Raes, D., Smith, M., Crop Evapotranspiration: Guidelines for Computing Crop Water Requirements. United Nations Food and Agriculture Organization, *Irrigation and Drainage Paper 56*, Rome, Italy, 300 pp, 1998.

Arora V.K., The use of the aridity index to assess climate change effect on annual runoff, *J. of Hydrology*, 265, 164–177, 2002.

ASCE, *Evapotranspiration and Irrigation Water Requirements*, Jensen, M.E., R.D. Burman, and R.G. Allen (editors), ASCE Manuals and Reports on Engineering Practice No. 70, 1990.

Avon, L. and T.J. Durbin, Evaluation of the Maxey-Eakin Method for Estimating Recharge to Ground-Water Basins in Nevada, *Water Resources Bulletin*, 30, (1), 99–111. Herndon, Virginia: American Water Resources Association, 1994.

Ball R.A., L.C. Purcell and S.K. Carey, Evaluation of solar radiation prediction models in North America. *Agron. J.* 96:391–397, 2004.

Bodvarsson, G.S., C.K. Ho, and B.A. Robinson (eds.), Preface. Special issue: Yucca Mountain Project, *J. Contam. Hydrol.*, 62–63:1–2, 2003a.

Bodvarsson, G.S., E. Kwicklis, C. Shan, and Y.S. Wu, Estimation of Percolation Flux from Borehole Temperature Data at Yucca Mountain, Nevada, *Journal of Contaminant Hydrology, 62–63,* 3–22. New York, New York: Elsevier, 2003b.

Brubaker, K.L. and D. Entekhabi, Analysis of feedback mechanisms in land-atmosphere interaction. Water Resour. Res. 32(5), 1343, 1996.

Brutsaert, W., *Evaporation into the Atmosphere: Theory, History, and Applications*, D. Reidel Publishing Company, Dordrecht, Holland, 1982.

BSC (Bechtel SAIC Company). *Future Climate Analysis.* ANL-NBS-GS-000008, Rev. 01. Las Vegas, Nevada: Bechtel SAIC Company, 2004a.

BSC (Bechtel SAIC Company), *Yucca Mountain Site Description.* TDR-CRW-GS-000001 REV 02 ICN 01. Two volumes. Las Vegas, Nevada: Bechtel SAIC Company. ACC, 2004b.

Budyko, M. I., *Evaporation under natural conditions*. GIMIZ, Leningrad, 1948. (IPST translation, Jerusalem, 1963.)

Budyko, M.I., On climatic factors of runoff. *Probl. Fiz. Geogr.,* 16, 1951.

Budyko, M.I., *Climate and Life*, Academic, San Diego, Calif., 508 pp., 1974.

Budyko, M.I., and L.I. Zubenok, The determination of evaporation from the land surface. Izv. *Akad. Nauk SSSR Ser. Geogr.*, 6, 3-17, 1961.

Cavazos, T., A.C. Comrie, and D.M. Liverman, Intraseasonal variability associated with wet monsoons in Southeast Arizona, *Journal of Climate*, 15(17), 2477-2490, 2002.

CRWMS M&O, *Engineering Design Climatology and Regional Meteorological Conditions Report.* B00000000-01717-5707-00066 REV 00. Las Vegas, Nevada: CRWMS M&O, 1997a.

CRWMS M&O, *Unsaturated Zone Flow Model Expert Elicitation Project.* Las Vegas, Nevada: CRWMS M&O. ACC: MOL.19971009.0582, 1997b.

Czarnecki, J.B., Simulated Effects of Increased Recharge on the Ground-Water Flow System of Yucca Mountain and Vicinity, Nevada-California. USGS-WRI-84-4344. Water-Resources Investigations Report, U.S. Geological Survey, 1985.

Davisson, M.L., and T.P. Rose, A Calibrated Maxey-Eakin Curve for the Fenner Basin of the Eastern Mojave Desert, California, LLNL, Report UCRL-ID-139030, 2000.

D'Agnese, F.A., C.C. Faunt, A.K. Turner, and M.C. Hill, *Hydrogeologic Evaluation and Numerical Simulation of the Death Valley Regional Ground-Water Flow System, Nevada and California.* Water-Resources Investigations Report 96-4300. Denver, Colorado: U.S. Geological Survey, 1997.

Donovan, D.J. and T. Katzer, Hydrologic Implications of Greater Ground-Water Recharge to Las Vegas Valley, Nevada. *Journal of the American Water Resources Association*, 36, 5, 1,133–1,148. Herndon, Virginia: American Water Resources Association, 2000.

Dooge, J. C. I., Modelling the behaviour of water, In: Reynolds, E. R. C. and F.B.Thompson (eds.), *Forests, Climate, and Hydrology: Regional Impacts*, The United Nations University, 1988.

Douglas, M. W., R. A. Maddox, K. Howard, and S. Reyes, The Mexican Monsoon, *Journal of Climate, 6,* 1665-1677, 1993.

Federer, C.A., C. Vörösmarty, and B. Fekete. Intercomparison of methods for calculating potential evaporation in regional and global water balance models. *Water Resour. Res.*, 32, 2315-2321, 1996.

Fisher, J.B., T.A. DeBiase, Y. Qi, M. Xu, and A.H. Goldstein, Evapotranspiration models compared on a Sierra Nevada forest ecosystem. *Environmental Modeling & Software*, 20(6), 783-796, 2005.

Hargreaves, G.H. and Z.A. Samani, Estimating potential evapotranspiration. *J. Irrig. and Drain Engr.*, ASCE, 108(IR3), 223-230, Hargreaves, G.H. and Z.A. Samani 1982. Estimating potential evapotranspiration. J. Irrig. and Drain Engr., ASCE, 108(IR3):223-230.

Harrill, J.R. and Prudic, D.E. *Aquifer Systems in the Great Basin Region of Nevada, Utah, and Adjacent States - Summary Report.* Professional Paper 1409-A. Denver, Colorado: U.S. Geological Survey, 1998.

Hatfield, J.L., and R.G. Allen, Evapotranspiration estimates under deficient water supplies. *J. Irrig. Drain. Eng.* 122(5), 301–308, 1996.

Konx, J.B., Global climate change: Impacts on California. An introduction and overview. In: Knox, J.B. and A.F. Scheuring (Eds.), *Global Climate Change and California: Potential Impacts and Responces*, University of California Press, Berkeley, California, 1-25, 1991,

Lichty, R.W. and P.W. McKinley, *Estimates of Ground-Water Recharge Rates for Two Small Basins in Central Nevada.* Water-Resources Investigations Report 94-4104, U.S. Geological Survey, Denver, Colorado, 1995.

Linacre, E.T., Estimating U.S. Class A pan evaporation from few climate data. *Water International,* 19, 5-14, 1994.

Liu, J., E.L. Sonnenthal, and G.S. Bodvarsson, Calibration of Yucca Mountain Unsaturated Zone Flow and Transport Model Using Porewater Chloride Data, *Journal of Contaminant Hydrology, 62–63,* 213–235. New York, New York: Elsevier, 2003.

Lu, J., G. Sun, S.G. McNulty, and D. M. Amatya, A Comparison of Six Potential Evapotranspiration Methods for Regional Use in the Southeastern United States, *Journal of the American Water Resources Association*, 41(3), 621-633, 2005.

Manabe, S., Climate and the Ocean Circulation: I. The Atmospheric Circulation and the Hydlrology of the Earth's Surface, *Monthly Weather Review*, 97, No. 11, Nov. 1969.

Mather, J.R., *The Climatic Water Budget in Environmental Analysis.* Lexington Books, Lexington MA, 239pp., 1978.

Maurer, D.K., and D. L. Berger, Subsurface flow and water yield from watersheds tributary to Eagle Valley hydrographic area, west-central Nevada, *U.S. Geological Survey Water-Resources Investigation Report 97-4191*, 1997.

Maxey, G.B. and Eakin, T.E., *Ground Water in White River Valley, White Pine, Nye, and Lincoln Counties, Nevada.* Water Resources Bulletin No. 8. Carson City, Nevada: State of Nevada, Office of the State Engineer, 1950.

Milly, P.C.D., Climate, soil water storage, and the average annual water balance. *Water Resour. Res.* 30 (7), 2143–2156, 1994.

Milly P. C. D. and K. A. Dunne, Macroscale water fluxes: 2. Water and energy supply control of their interannual variability, *Water Resour. Res.*, 38(10), 1206, 2002.

Milly, P. C. D., and A.B. Shmakin, Global Modeling of Land Water and Energy Balances, Part II: Land-Characteristic Contributions to Spatial Variability, *Journal of Hydrometeorology*, 3(3), 301-310.

Mintz, Y., and G.K. Walker, Global Fields of Soil Moisture and Land Surface Evapotranspiration Derived from Observed Precipitation and Surface Air Temperature, *J. Applied. Meteor.*, 32, 1305-1334, 1993.

Mintz, Y., and Serafini, Y.V., A Global Monthly Climatology of Soil Moisture and Water Balance, *Climate Dynamics*, 8, 13-27, 1992.

Muller, R.A. and G.J. MacDonald, *Ice Ages and Astronomical Causes*, Springer Praxis, Chichester, UK, 2000.

NAM—*National Agronomy Manual*, USDA-NRCS, part 502.33, 2002.

Ol'dekop, E.M., 1911. On evaporation from the surface of river basins. *Trans. Met. Obs. lur-evskogo*, Univ. Tartu 4 in Russian. (Reference in Arora, 2002).

Penman, H.L., Natural Evaporation from Open Water, Bare Soil and Grass, *Proc. R. Soc. London*, Ser. A, 193, 120-145, 1948.

Petit, J.R., J. Jouzel, D. Raynaud, N.I. Barkov, J.-M. Barnola, I. Basile, M. Bender, J. Chappellaz, M. Davis, G. Delayque, M. Delmotte, V.M. Kotlyakov, M. Legrand, V.Y. Lipenkov, C. Lorius, L. Pépin, C. Ritz, E. Saltzman, and M. Stievenard, Climate and atmospheric history of the past 420,000 years from the Vostok ice core, Antarctica. *Nature* 399: 429-436, 1999.

Pike, J. G., The estimation of annual runoff from meteorological data in a tropical climate, *J. Hydrol.*, 2, 116– 123, 1964.

Ponce, V.M., Pandey, R.P., Ercan, S., Characterization of drought across the climate spectrum. *J. Hydrol. Engng*, ASCE 5 (2), 222–224, 2000.

Potter, N. J., L.Zhang, P.C.D. Milly, T.A. McMahon, and A.J.Jakeman, Effects of rainfall seasonality and soil moisture capacity on mean annual water balance for Australian catchments, *Water Resour. Res.* 41, W06007, 2005.

Priestley, C.H.B., and R.J. Taylor, On the Assessment of Surface Heat Flux and Evaporation Using Large-Scale Parameters, *Monthly Weather Review*, 100, No. 2, 81-92, February 1972.

Rasmusson, E.M., A study of the hydrology of Eastern North America using atmospheric vapor flux data, *Monthly Weather Review,* Vol. 99, No. 2, pp. 119–135, 1971.

Rosenberg, N.J., Blad, B.L. & Verma, S.B. *Microclimate in the Biological Environment.* 2nd ed. New York NY: John Wiley & Sons. 495p., 1983.

Sankarasubramanian A. and R.M. Vogel, Hydroclimatology of the continental United States, *Geophysical Research Letters,* 30(7), 1363, 2003.

Scanlon, B. R., S.W. Tyler, and P.J. Wierenga, Hydrologic issues in arid, unsaturated systems and implications for contaminant transport, *Reviews of Geophysics*, 35(4), 461–490, 1997.

Sharif, H., and N. L. Miller, Hydroclimatological predictions based on basin's Humidity Index, Extended Abstract, Joint with 18th Conference on Climate Variability and Change and 20th Conference on Hydrology, January 2006.

Schreiber, P., U¨ ber die Beziehungen zwischen dem Niederschlagund der Wasserfu¨hrung der Flu¨ße in Mitteleuropa. Z. Meteorol. 21 (10), 441–452, 1904. (Reference in Arora, 2002).

Sharpe, S., *Future Climate Analysis—10,000 Years to 1,000,000 Years After Present.* MOD-01-001 REV 00. [Reno, Nevada]: Desert Research Institute. ACC: MOL.20020422.0011, 2002.

Sharpe, S., *Future Climate Analysis—10,000 Years to 1,000,000 Years After Present.* MOD-01-001 REV 01. [Reno, Nevada: Desert Research Institute], 2003.

Shuttleworth, W.J., and I.R. Calder, Has the Priestley-Taylor equation any relevance to the forest evaporation? *Journal of Applied Meteorology*, 18, 639-646, 1979.

Shuttleworth, W.J. and Wallace, J.S., Evaporation from sparse crops: An energy combination theory, *Quarterly J. Royal Meteorol. Soc.*, 111, 839-855, 1985.

Spaulding, W.G., Vegetation and climates of the last 45,000 years in the vicinity of the Nevada Test Site, south-central Nevada. U.S. Geological Survey Professional Paper 1329. 83 p., 1985.

Stagnitti, F., Parlange, J.-Y. and Rose, C.W., Hydrology of a small wet catchment. *Hydrol. Sci.*, 3: 137-150, 1989.

Steenhuis, T.S. and W.H. Van der Molen, The Thornthwaite-Mather procedure as a simple engineering method to predict recharge. *J. Hydrol.* 84:221-229, 1986.

Thom, A.S., J.L.Thony, and M.Vauclin, On the proper employment of evaporation pans and atmometers in estimating potential transpiration. *Quarterly J. Royal Meteorol. Soc.*, 107, 711-736, 1981.

Thompson, R.S., K.H.Anderson, and P.J.Bartlein, *Quantitative Paleoclimatic Reconstructions from Late Pleistocene Plant Macrofossils of the Yucca Mountain Region.* Open-File Report 99-338. Denver, Colorado: U.S. Geological Survey. 1999.

Thornthwaite, C.W., The Climates of North America According to a New Classification. *Geog. Review*, 21, 633-655, 1931.

Thornthwaite, C.W. and J.R. Mather, *The Water Balance*. Laboratory of Climatology, No. 8, Centerton, NJ, 1955.

Thornthwaite, C.W., An approach toward a rational classification of climate, *Geographical Review*, 38, 55-94, 1948.

Turc, L., Le bilan d'eau des sols: Relation entre les pre´cipitations, l'e´vaporation et l'e´coulement, Ann. Agron., 5, 491– 569, 1954. Reference in Brutsaert, 1982.

USGS, *Future Climate Analysis.* ANL-NBS-GS-000008 REV 00 ICN 01. Denver, Colorado: U.S. Geological Survey. ACC: MOL.20011107.0004, 2001.

Xu, T., E. Sonnenthal, and G. Bodvarsson, A Reaction-Transport Model for Calcite Precipitation and Evaluation of Infiltration Fluxes in Unsaturated Fractured Rock. *Journal of Contaminant Hydrology*, 64, (1–2), 113–127. New York, New York: Elsevier. 2003.

Walvoord, M.A., D.A. Stonestrom, and F.M. Phillips, From multi-year observations to millennial inferences: Uncertainties in paleohydrologic reconstructions of deep unsaturated zones in the desert southwest. *Eos Trans. AGU, 83*(47), Fall Meet. Suppl., Abstract H22F-07, 2002a.

Walvoord, M.A., M.A.Plummer, F.M.Phillips, and A.V.Wolfsberg, Deep arid system hydrodynamics: 1. Equilibrium states and response times in thick desert vadose zones, *Water Resour. Res.*, 38(12), 1308, 2002b.

Willmott, C.J., C.M. Rowe, and Y. Mintz, Climatology of the Terrestrial Seasonal Water Cycle, *Journal of Climatology*, 5, 589-606, 1985.

Wilson, J.L., and H. Guan, Mountain-block hydrology and mountain-front recharge, in *Groundwater Recharge in a Desert Environment: The Southwestern United States*, (eds. J.F. Hogan, F.M. Phillips, and B.R. Scanlon), Water Science and Applications Series, vol. 9, American Geophysical Union, Washington, D.C., 113-137, 2004.

Winograd, I.J., Coplen T.B., Landwehr, J.M., Riggs, A.C., Ludwig,K.R., Szabo, B.J., Kolesar, P.T., and Revesz, K.M., Continuous 500,000-year climate record from vein calcite in Devils Hole, Nevada: *Science*, 258, 255-260, 1992.

Winograd, I.J. and W. Thordarson, *Hydrogeologic and Hydrochemical Framework,South-Central Great Basin, Nevada-California, with Special Reference to the Nevada Test Site.* Geological Survey Professional Paper 712-C. Washington, D.C.: United States Government Printing Office, 1975.

Wright, W. E., A. Long, A. C. Comrie, S. W. Leavitt, T. Cavazos, and C. Eastoe, 2001: Monsoonal moisture sources revealed using temperature, precipitation and precipitation stable isotope timeseries. *Geophys.Res. Lett.*, 28, 787–790, 2001.

Zhang, L., W.R. Dawes, and G.R. Walker, Response of mean annual evapotranspiration to vegetation changes at catchment scale. *Water Resour. Res.*, 37 (3), 701-708, 2001.

Zhu, C., Estimate of recharge from radiocarbon dating of groundwater and numerical flow and transport modeling, Water Resour. Res., 36(9), 2607–2620, 2000.

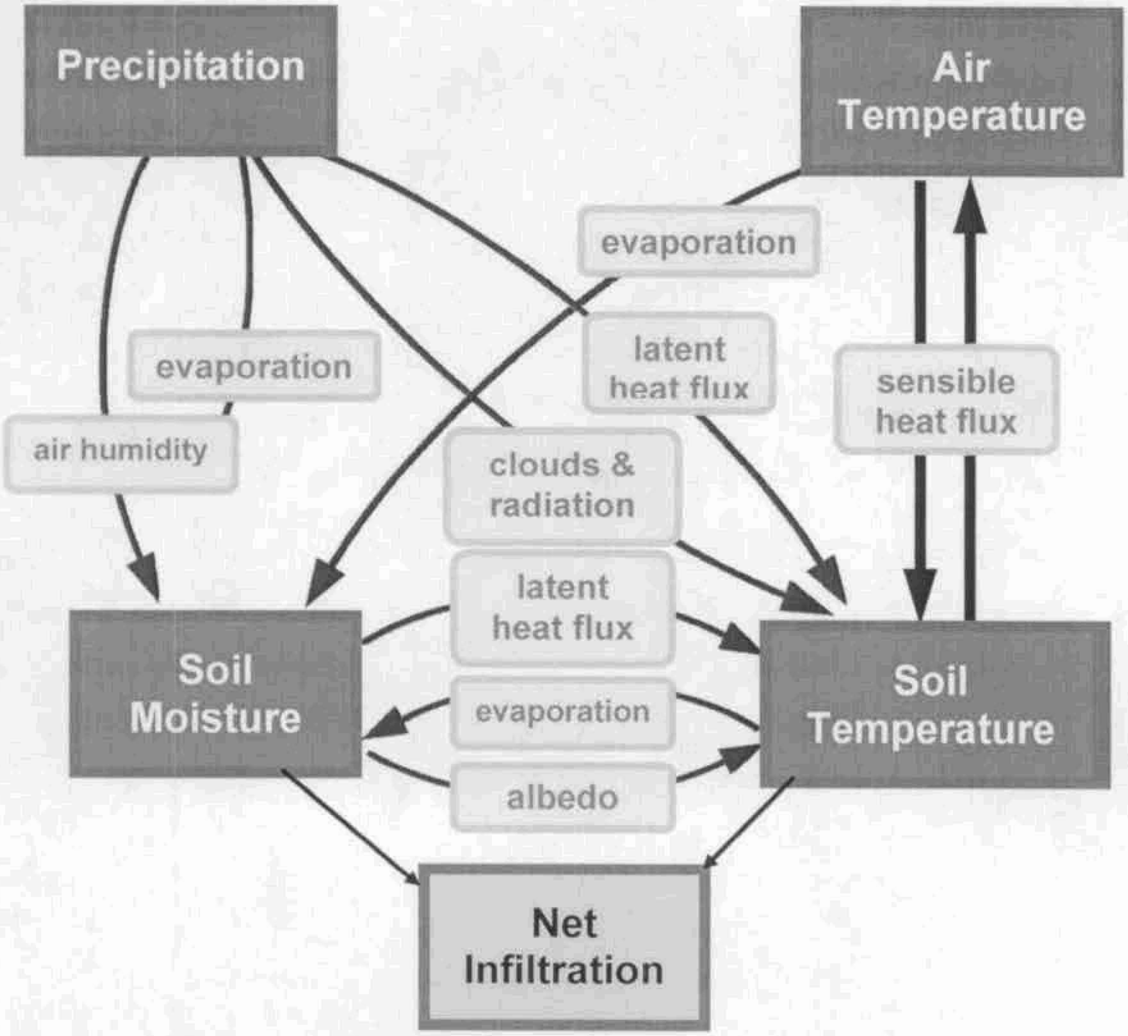

Figure 1. Schematic showing the relationship between dominant meteorological parameters affecting water and energy transfer in an atmospheric-shallow subsurface system, including net infiltration (modified from Brubaker and Entekhabi, 1996).

Source: Sharpe 2003 [DIRS 161591], Figure 6-3, p. 30

Figure 2. Locations of the Yucca Mountain Analogue Meteorological Stations (Sharpe, 2003).

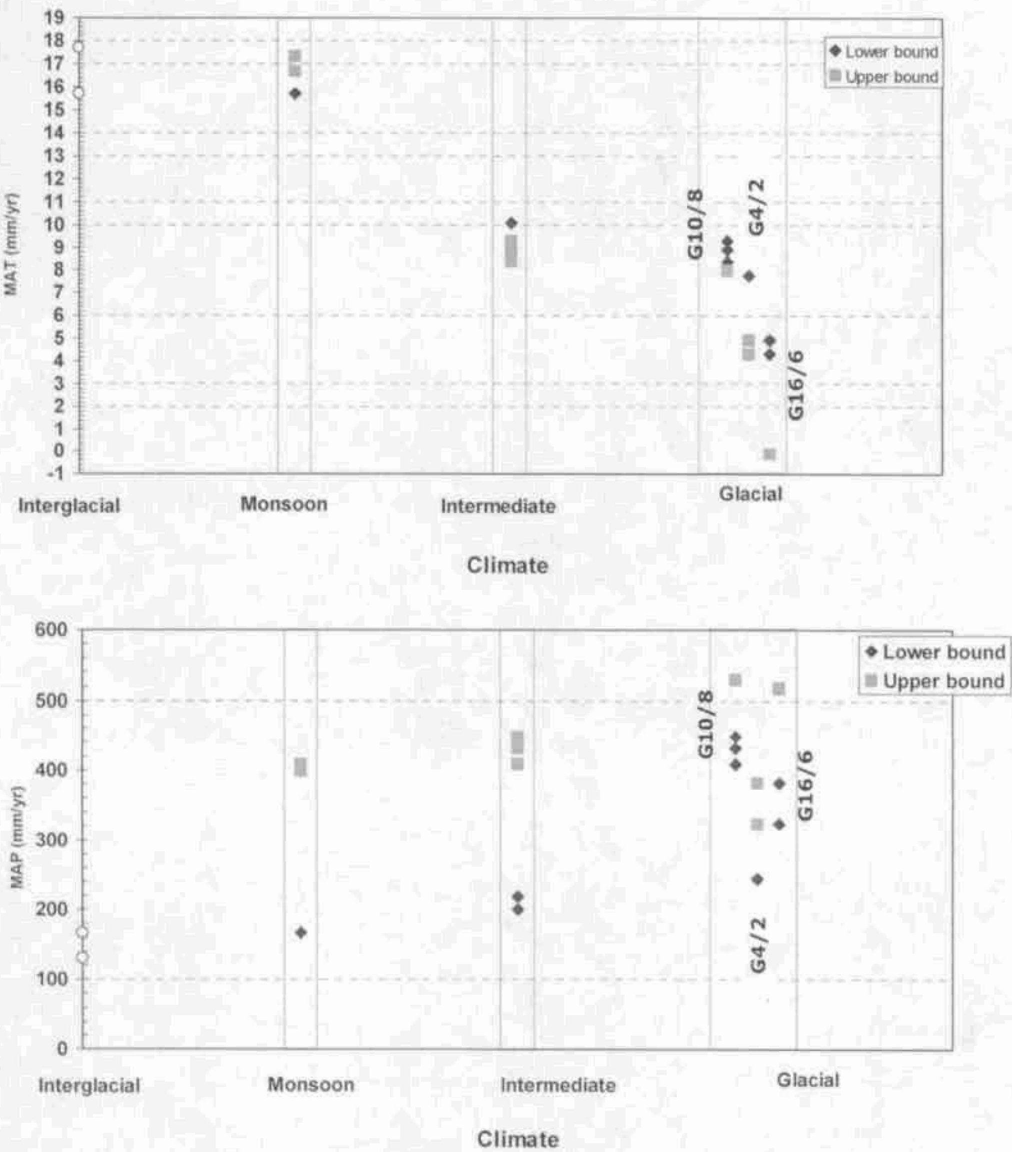

Figure 3. Changes in the mean annual temperature (MAT) and the mean annual precipitation (MAP), using data from analogue meteorological stations. Note: open circles are for the MAT and MAT interglacial (present-day) climate, using the data from the Yucca Mountain meteorological sites 2 and 5.

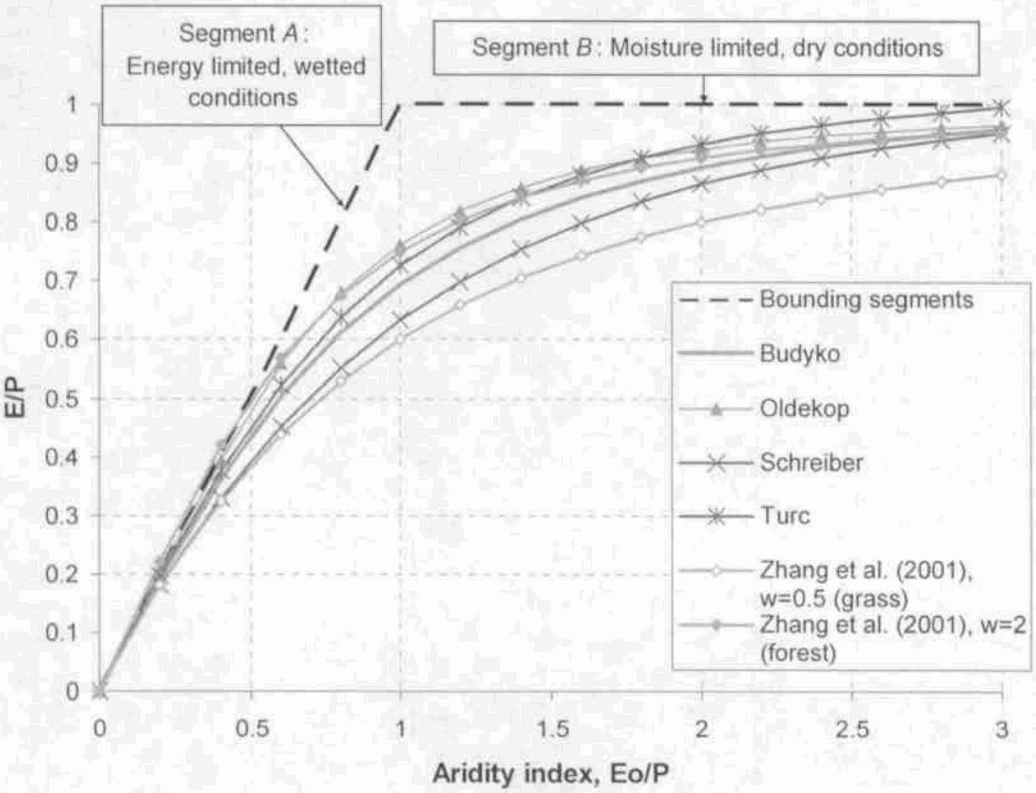

Figure 4. Plots of the relationship between E/P and the aridity index (E_o/P) calculated from different semi-empirical formulae, illustrating that Budyko's curve (Equation 6) is in the middle of curves from other formulae.

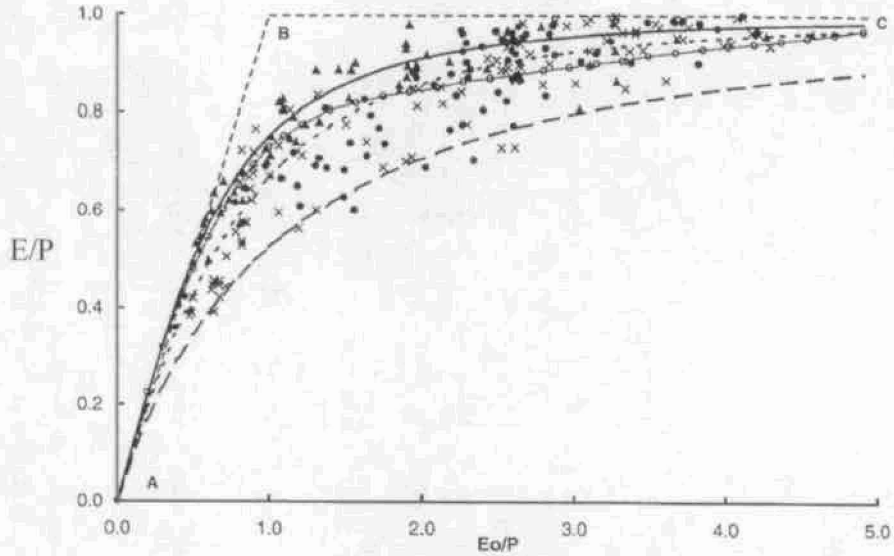

Figure 5. Comparison of experimental data (forest, mixed, and pasture) from Zhang et al. (2001) with analytical curves by Zhang et al. (2001, Eq.6) and Milly's (1994). Zhang et al. (2001) curves: solid line—w=2.0, small dashed line—w=1.0, and large dashed line—w=0.5. Milly's curve: solid line with open circles. Experimental data: triangles—forest, solid circles—mixed vegetation, and x—pasture.

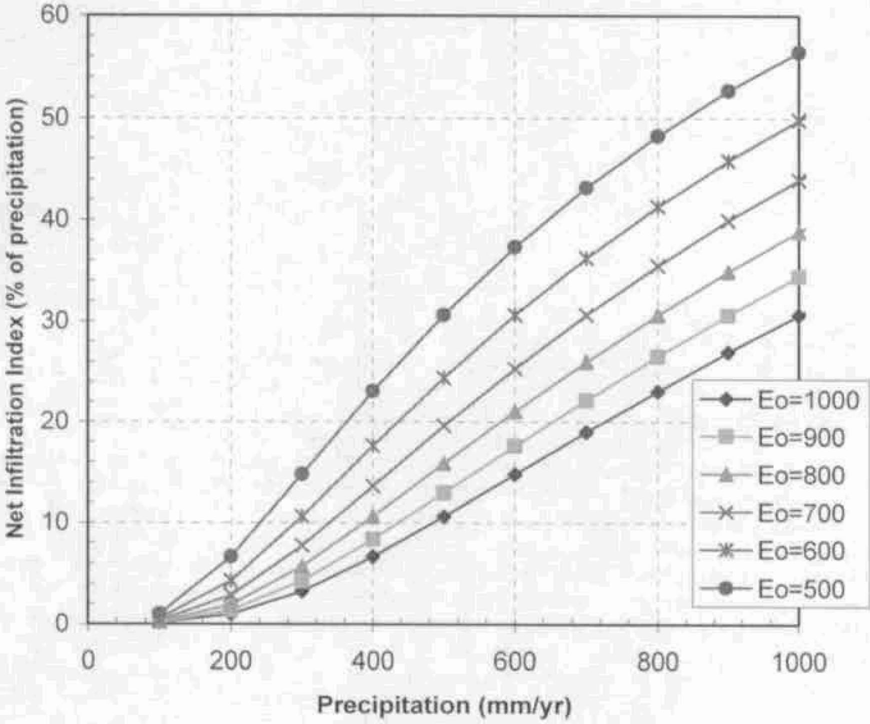

Figure 6. Net infiltration index (net infiltration given as percentage of precipitation) for different reference potential evapotranspiration E_0 rates (mm/yr), calculated from the Budyko model.

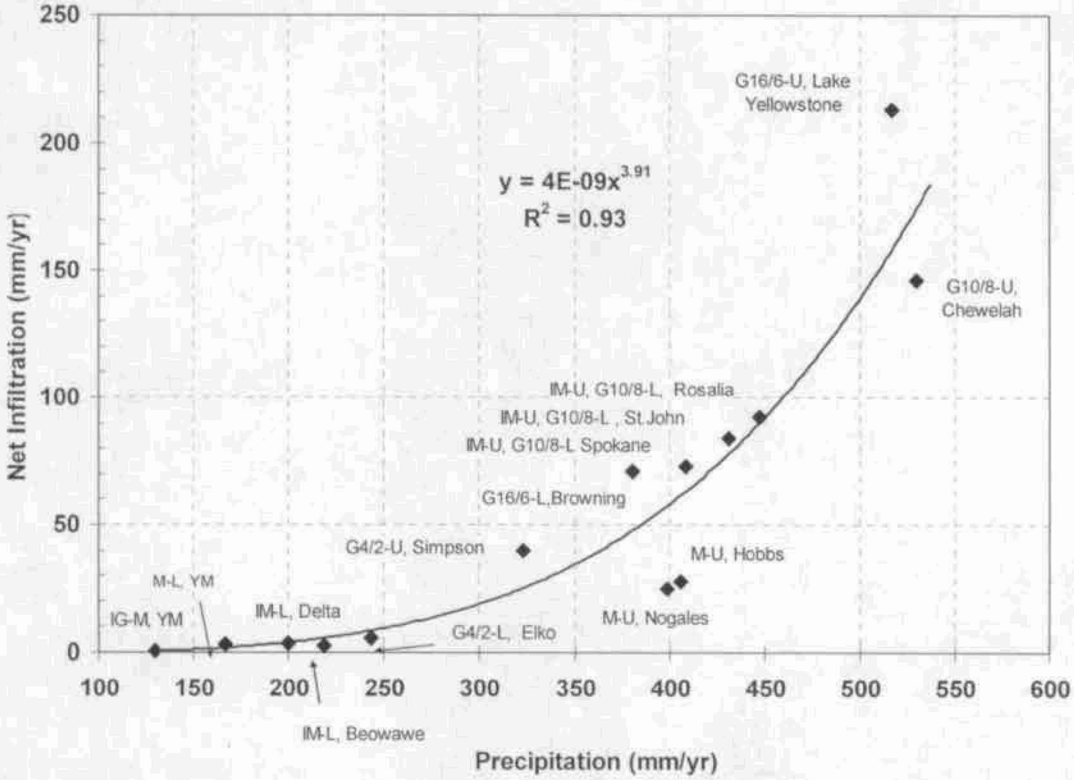

Figure 7. Relationship between calculated net infiltration and precipitation, showing the names of analogue meteostations and climates. Black dots are the forecasted data and the power-law regression line—Equation (16).

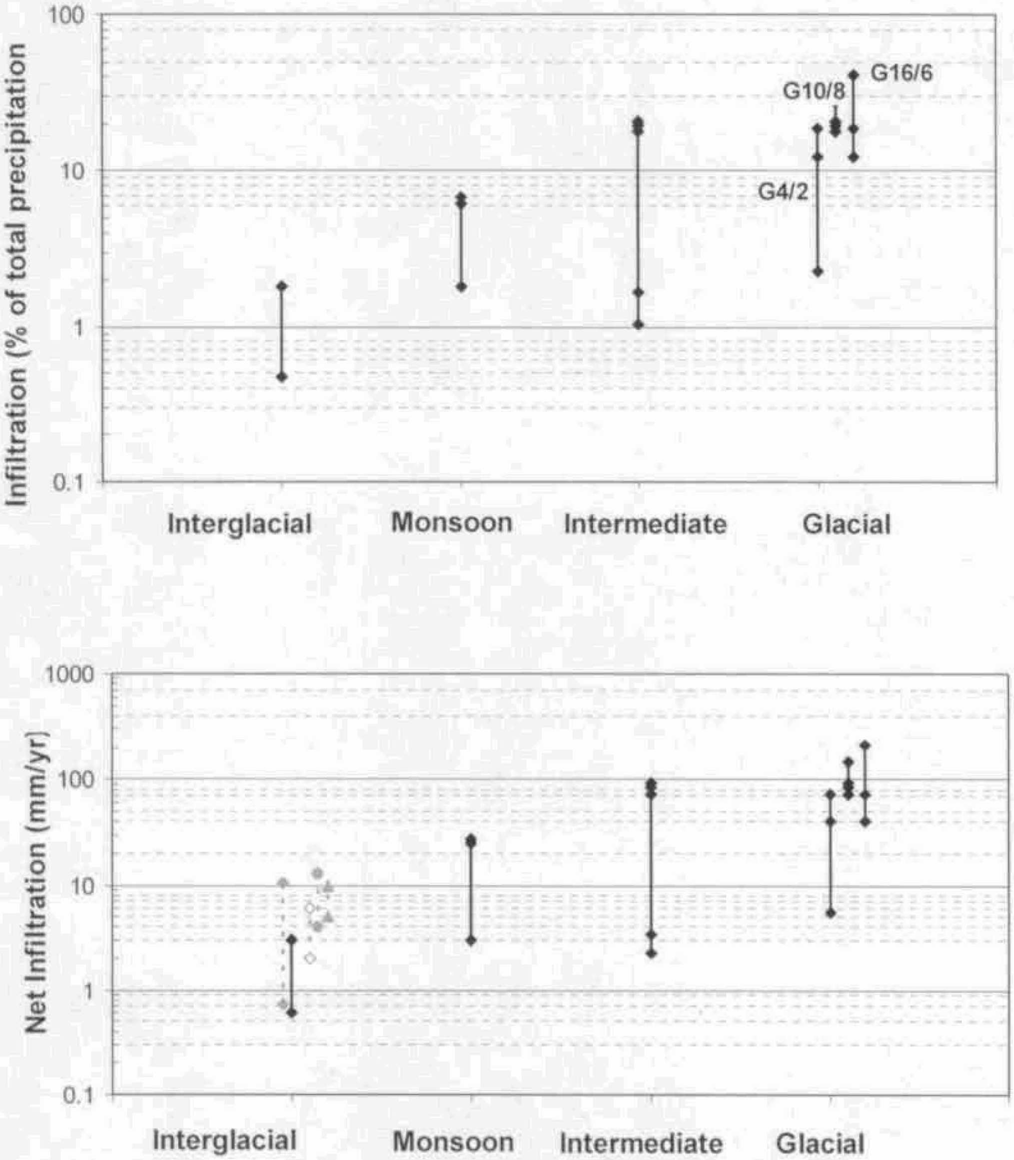

Figure 8. Ranking of ranges of forecasted net infiltration index (upper panel), and net infiltration (lower panel) for different climates. On the lower panel, for the present-day (interglacial) climate, red dashed lines show the ranges of the percolation flux from calculations using a chloride-mass balance model (solid diamonds), calcite-mass model (open diamonds), temperature data (closed circles), and experts' evaluation (solid triangles)—the references are given in the text.

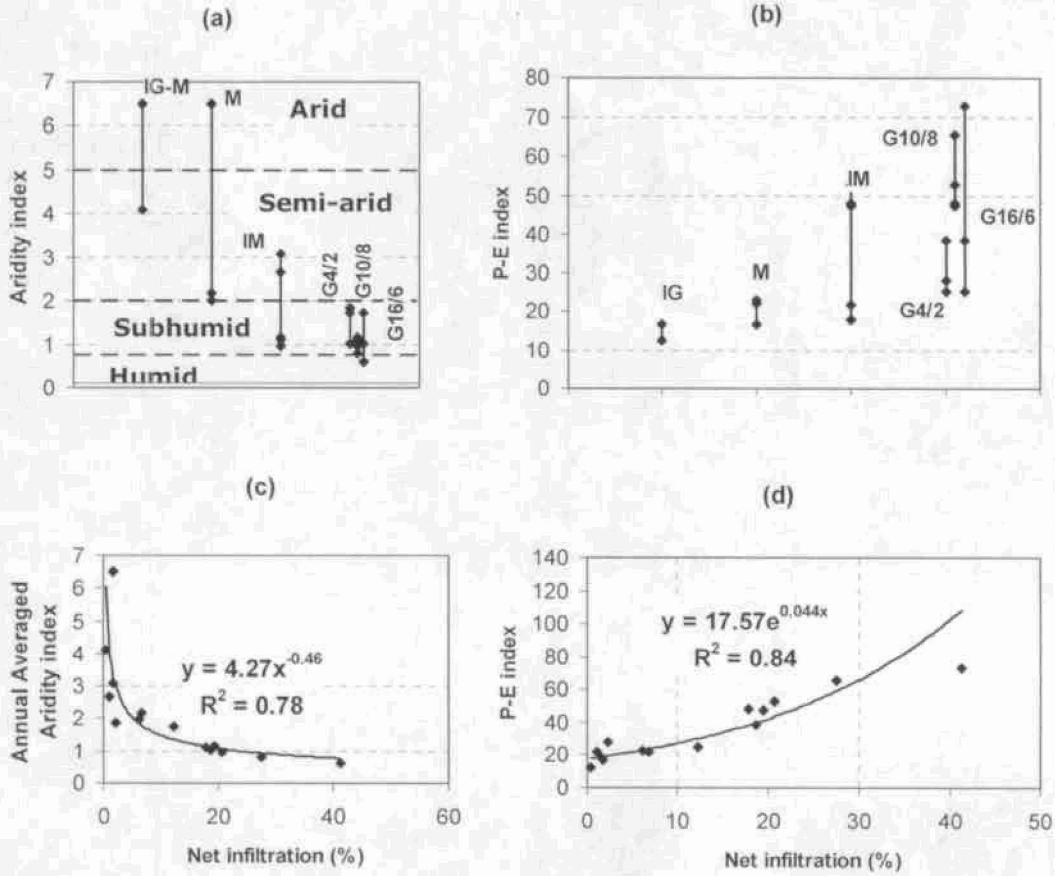

Figure 9. Climatic ranking of the annual average aridity index (a), P-E index (b). and the relationships of the aridity index vs. net infiltration index (c), and the P-E index vs. net infiltration index (d).

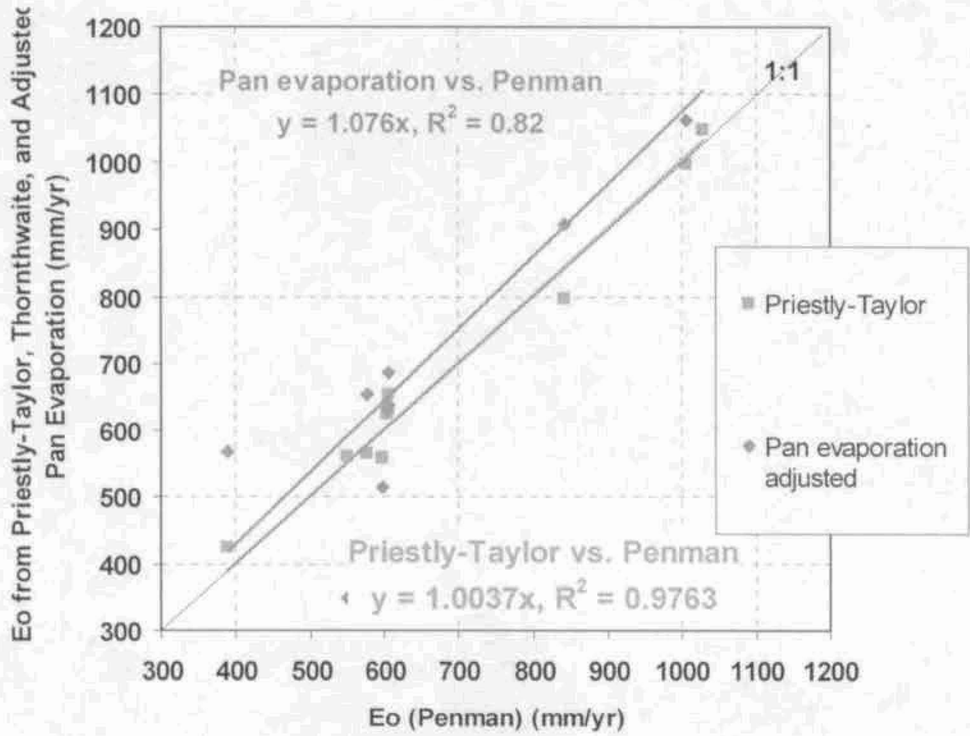

Figure 10. Correlation between the results of calculations of E_0 using Penman (1948) model with those from Priestly-Taylor equation and adjusted pan evaporation from Class A evaporometers.

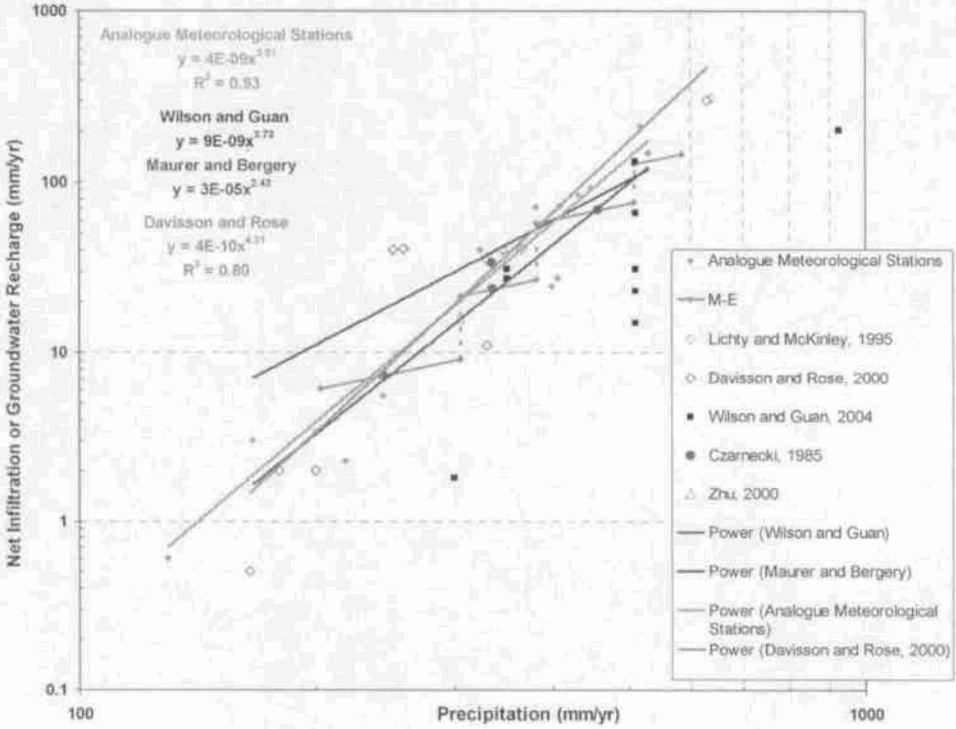

Figure 11. Comparison of climatic forecasting of net infiltration vs. precipitation with the groundwater recharges from published data—Maxey and Eaking (1950), Wilson and Guan (2004), Maurer and Berger (1997), Lichty and McKinley (1995), Davisson and Rose (2000), Czarnecki (1985), and Zhu (2000).

Table 1. Total Duration of the Interglacial (Present-Day) and Future Climate Stages over the Past 529,000 years, calculated from the data by Sharpe (2003)

Climate	Interglacial (Present-Day)	Monsoon	Intermediate (Glacial Transition)	Glacial				Total Duration
				G 10/8	G 4/2	G 16/6	Total Glacial	
Duration (yrs)	76,000	18,000	330,000	44,000	38,000	13,000	95,000	519,000
Duration (% of time)	14.64	3.47	63.58	8.48	7.32	2.50	18.30	100

Table 2. Types of Meteorological Data and Periods of Records from Analogue Meteorological Stations

Meteorological Stations	Temperature Max	Temperature Min	Temperature Mean	Dewpoint Temperature	Wind	Solar Radiation	Total Precipitation	Pan Evaporation
YM Site 2(*)	1986-1996	1986-1996	1986-1996	Calculated (**)	1993-1996	Calculated (***)	1986-1996	n/a
YM Site 5(*)	1986-1996	1986-1996	1986-1996	Calculated (**)	1993-1996	Calculated (***)	1986-1996	n/a
Hobbs	1914-2005	1914-2005	1914-2006	1950-2002	1992-2002	Calculated (***)	1914-2005	1914-2005
Beowawe	1949-2005	1949-2005	1949-2006	Calculated (**)	Elko	Elko	1949-2005	Beowawe (UofN Ranch)
Elko	1890-2005	1890-2005	1890-2006	1950-2002	1992-2002	1961-1990	1890-2005	Beowawe (UofN Ranch)
Nogales	1892-1948	1892-1948	1892-1948	Nogales	Nogales 6A	Tuscon AP	1892-1948	Nogales AP
Delta	1938-2005	1938-2005	1938-2006	Calculated (**)	1992-2002, Milford Airport	Calculated (***)	1938-2005	1960-2005, Fish Spring Refuge
Chewelah	1948-2005	1948-2005	1948-2006	Calculated (**)	1992-2002, Deer Park AP	Calculated (***)	1948-2005	1989-2005
Browning	1894-1989	1894-1989	1894-1989	1950-2002, Cut Bank	1992-2002, Cut Bank	1961-1990, Cut Bank	1894-1989	1948-2005, Babb 6
Rosalia	1948-2005	1948-2005	1948-2006	1950-2002, Spokane	1992-2002, Spokane-Fairchild AFB	1961-1990, Spokane	1948-2005	1989-2005
Simpson	1948-2005	1948-2005	1948-2006	1950-2002, Havre	1992-2002, Cut Bank	1961-1990, Spokane	1948-2005	1917-2005, Fort Assinniboine
Spokane	1890-2005	1890-2005	1889-2006	1950-2002	1992-2002, Spokane-Fairchild AFB	1961-1990, Spokane	1890-2005	1989-2005
St John	1963-2005	1963-2005	1963-2006	1950-2002, Spokane	1992-2002, Pullman-Moscow AP	1961-1990, Spokane	1963-2005	1989-2005, Spokane
Yellowstone	1948-2005	1914-2005	1914-2006	1950-2002	1992-2002	Calculated (***)	1948-2005	n/a

(*) Source: CRWMS M&O, 1997a, (**) Calculated from formula Tdew=Tmin-2 (T is in oC) (Allen et al., 1998), (***) Solar radiation calculated using Hargreaves formula (Hargreaves and Samani, 1982), taking into account the elevation of meteorological stations (Ball et al., 2004)

Table 3. Results of Calculations of E_0 and Net Infiltration for Analogue Meteorological Stations

Meteorological Station	Climate	Average Annual Temperature (°C)	Total Precipitation (mm/yr)	Eo (mm/yr)	Net Infiltration (mm/yr)	Net Infiltration Index (% of Total Precipitation)	*P-E* Index	Aridity Index
YM Site 2	IG-M	15.70	166.62	682.70	3.00	16.42	16.42	6.49
YM Site 5	IG-M	17.70	129.54	841.31	0.61	12.256	12.256	4.10
YM Site 2	M-L	15.70	166.62	841.31	3.00	16.42	16.42	6.49
Nogales, AZ	M-U	17.29	398.78	1028.73	24.58	22.89	22.89	2.00
Hobbs, NM	M-U	16.63	405.89	1005.57	27.45	21.89	21.89	2.18
Delta, UT	IM-L	10.07	200.15	841.35	3.34	17.91	17.91	3.08
Beowawe, NV	IM-L	8.88	218.44	1078.33	2.26	21.57	21.57	2.65
St.John, WA	IM-U	9.28	431.29	606.62	83.80	47.23	47.23	1.16
Spokane, WA	IM-U	8.89	408.43	607.09	72.89	47.98	47.98	1.10
Rosalia, WA	IM-U	8.36	447.29	603.46	92.46	52.62	52.62	0.96
Elko WB airport, NV	G 4/2-L	7.78	243.59	923.97	5.49	27.87	27.87	1.85
Simpson 6NW, MT	G 4/2-U	4.93	323.34	597.38	39.85	24.95	24.95	1.74
Browning, MT	G 4/2-U	4.31	380.75	549.81	71.07	38.41	38.41	1.02
St.John, WA	G 10/8-L	9.28	431.29	606.62	83.80	47.23	47.23	1.16
Spokane, WA	G 10/8-L	8.89	408.43	607.09	72.89	47.98	47.98	1.10
Rosalia, WA	G 10/8-L	8.36	447.29	603.46	92.46	52.62	52.62	0.96
Chewelah, WA	G 10/8-U	7.97	530.10	578.04	146.18	65.43	65.43	0.79
Simpson 6NW, MT	G 16/6-L	4.93	323.34	597.38	39.85	24.95	24.95	1.74
Browning, MT	G 16/6-L	4.31	380.75	549.81	71.07	38.41	38.41	1.02
Lake Yellowstone, WY	G 16/6-U	-0.12	516.89	388.77	213.03	72.68	72.68	0.60